JOURNAL OF AGRICULTURAL AND FOOD CHEMISTRY
ARTICLE

J. Agric. Food Chem. 2009, 57, 3949–3954 3949
DOI:10.1021/jf9001704

Absorption of 3(2*H*)-Furanones by Human Intestinal Epithelial Caco-2 Cells

Nicole Christina Stadler,[†] Veronika Somoza,[‡] and Wilfried Schwab*,[†]

[†]Biomolecular Food Technology, Technical University München, Hochfeldweg 1, 85354 Freising, Germany, and [‡]Department of Food Science, University of Wisconsin—Madison, A103 Babcock Hall, Madison, Wisconsin 53706

A number of 3(2*H*)-furanones are synthesized by fruits and have been found in cooked foodstuffs, where they impart flavor and odor because of their low perception thresholds. They show genotoxic properties in model studies but are also ranked among the antioxidants and anticarcinogens. This study examined the efficiency of intestinal absorption and metabolic conversion of 3(2*H*)-furanones by using Caco-2 cell monolayers as an intestinal epithelial cell model. The permeability of each agent was measured in both the apical to basal and basal to apical directions. 2,5-Dimethyl-4-methoxy-3(2*H*)-furanone (DMMF) showed the highest absorption rate in all experiments, while similar amounts of 4-hydroxy-2,5-dimethyl-3(2*H*)-furanone (HDMF), 4-hydroxy-2(or 5)-ethyl-5(or 2)-methyl-3(2*H*)-furanone (HEMF), and 4-hydroxy-5-methyl-3(2*H*)-furanone (HMF) were taken up. HDMF-glucoside was almost not absorbed but was hydrolyzed to a small extent. The transport of 3(2*H*)-furanones could not be saturated even at levels of 500 μM and occurred in both directions. Because the uptake was only slightly reduced by apical hyperosmolarity, passive diffusion by paracellular transport is proposed.

KEYWORDS: Furanones; furaneol; methoxyfuraneol; norfuraneol; homofuraneol; absorption; Caco-2; passive diffusion

INTRODUCTION

Fragrant 3(2*H*)-furanones, such as 4-hydroxy-2,5-dimethyl-3(2*H*)-furanone (HDMF), 4-hydroxy-2(or 5)-ethyl-5(or 2)-methyl-3(2*H*)-furanone (HEMF), and 4-hydroxy-5-methyl-3(2*H*)-furanone (HMF), have been found in a range of cooked foodstuffs, where they are formed as a result of the Maillard reaction between sugars and amino acids during heating (**Figure 1**, *1*). Because of their low odor threshold values, the 4-hydroxy-3(2*H*)-furanones and the metabolite 2,5-dimethyl-4-methoxy-3(2*H*)-furanone (DMMF) also contribute to the flavor of strawberry, raspberry, pineapple, tomato, and fermented foods (*2*, *3*). In fruit, HDMF, DMMF, and the glucoside of HDMF are enzymatically synthesized from carbohydrate phosphates during the late stages of ripening. Non-enzymatic formation of these compounds occurs through the Maillard reaction. During fermentation processes, furanones are probably formed by enzymatic and non-enzymatic reactions (*1*, *2*). High levels of up to 55 mg of HDMF/kg of fruit fresh weight are present in strawberry. Synthetic furanones and those extracted from natural sources are largely used by the food and beverage industry as additives, exhibiting caramel-like odor (*4*, *5*).

Furanones occurring in foods are also mutagenic and show cytotoxic effects on bacteria and some tumor cell lines (*6*−*8*). These effects may be related to a DNA-damaging activity (*9*−*11*). In animal trials, however, these compounds have been demonstrated to effectively act as dietary anticarcinogenic agents when animals were treated with known cancer-inducing compounds, such as benzo[*a*]pyrene (*12*, *13*). Besides, furanones act as reductants and are antioxidants because they inhibit hydroxyl and peroxyl radical-mediated lipid peroxidation by scavenging singlet oxygen and peroxyl radicals (*12*−*15*). HDMF shows also antimicrobial activity on various human pathogenic microorganisms and scavenge nitrous acid (*16*, *17*).

To clarify the relevance of the observed effects for humans, it is important to determine the absorption, distribution, metabolism, and excretion kinetics of furanones. First results from pharmacokinetic studies in rats and humans showed that, in rats, HDMF is the predominant furanone excreted in the urine, while HDMF-glucuronide has been identified as the major metabolite of HDMF in the urine of six volunteers (*18*, *19*). Results from the human intervention trail demonstrated that up to 94% of the furanones ingested were quantified in the urine by means of liquid chromatography−tandem mass spectrometry (LC−MS/MS) analysis (*19*). However, pharmacokinetic data among the volunteers showed considerable variation, and further work is needed.

In this study, the absorption of HDMF, DMMF, HDMF-glucoside, HEMF, and HMF by human intestinal epithelial Caco-2 cells was thoroughly analyzed. The absorption rates were determined, the transport mechanism was clarified, and the metabolism of the furanones in the test system was investigated by LC−MS.

*To whom correspondence should be addressed: Biomolecular Food Technology, Technische Universität München, Hochfeldweg 1, 85354 Freising, Germany. Telephone: +49(0)8161712912. Fax: +49(0)8161712950. E-mail: schwab@wzw.tum.de.

 Published on Web 4/1/2009

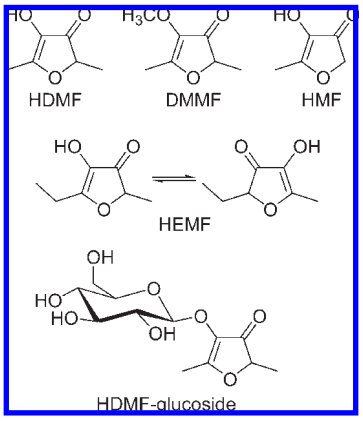

Figure 1. Structural formula: 4-hydroxy-2,5-dimethyl-3(2*H*)-furanone (HDMF), 2,5-dimethyl-4-methoxy-3(2*H*)-furanone (DMMF), 4-hydroxy-5-methyl-3(2*H*)-furanone (HMF), 4-hydroxy-2(or 5)-ethyl-5(or 2)-methyl-3(2*H*)-furanone (HEMF), and 4-hydroxy-2,5-dimethyl-3(2*H*)-furanosyl-β-D-glucopyranoside (HDMF-glucoside).

MATERIALS AND METHODS

Materials. HDMF, HEMF, HMF, and DMMF were obtained from Sigma-Aldrich, Steinheim, Germany. HDMF-glucoside was synthesized according to Mayerl et al. (*20*). Acetonitrile, methanol, formic acid, 2-propanol, mannitol, and trypan blue were purchased from Sigma-Aldrich, Steinheim, Germany.

Caco-2 Cell Cultures. Caco-2 cells were isolated from a differentiated adenocarcinoma of the colon of a 72-year-old patient and kindly provided by Degussa Food Bioactives, Freising, Germany. The cell line was obtained from the German Collection of Microorganisms and Cell Cultures (DSMZ, Braunschweig, Germany, ACC 169). The adherent Caco-2 cells were cultured in Dulbecco's modified Eagle's medium (DMEM, Invitrogen/Gibco, Carlsbad, CA), supplemented with 20% fetal bovine serum (Sigma-Aldrich, Steinheim, Germany) and 1% non-essential amino acid solution (Invitrogen/Gibco, Carlsbad, CA). The monolayer cultures were grown in a humidified atmosphere of 5% CO_2/95% air at 37 °C. Cells were subcultured every 3 or 4 days and harvested with 0.25% trypsin and 0.8 mM ethylenediaminetetraacetic acid (EDTA), resuspended, and seeded into a new culture dish. For all studies, Caco-2 cells were seeded in Falcon cell culture inserts (polyethylene terephthalate membrane, 0.4 μm pore size, BD Biosciences, San Jose, CA) in 12-well plates at a density of 1.2×10^5 cells/insert (1 mL/insert). The basolateral and apical compartments contained 2 and 1 mL of culture medium, respectively.

Incubation of Caco-2 Cells with 3(2*H*)-Furanones. Caco-2 cells at passage 4-10 were used for experiments 21 days post-seeding in the Falcon inserts. The transepithelial electrical resistance (TEER) value of the monolayers was measured with a Millicel-ERS instrument (Millipore Co., Bedford, MA, *21*). At a membrane area of 0.9 cm^2, a closed monolayer was assumed when a resistance value of greater than 150 Ω cm^2 was measured. The absence of monolayer holes was confirmed by microscopy (*22*). The inserts were washed twice with 500 μL of Hanks' buffered salt solution (HBSS) at pH 7.4 for 30 min in a CO_2 incubator. Substances were dissolved in HBSS and added on either the apical side of the inserts or the basolateral side, while the other side contained HBSS. After incubation at 37 °C, 100 μL samples were withdrawn at defined periods. At the end of the incubation period, the TEER value was determined and the remaining volume of buffer was collected. Cells were washed twice with phosphate-buffered saline (PBS) and harvested with 0.25% trypsin and 0.8 mM EDTA after incubation at 37 °C at 5% CO_2 for 7−10 min. Cell viability was determined by trypan blue staining. Cells were washed with HPSS and cell pellets as well as the samples stored at −80 °C until analysis.

LC−Photodiode Array Detector (DAD) Analysis. The 3(2*H*)-furanones were quantified by a Merck-Hitachi (Darmstadt, Germany) LC system equipped with a DAD using a reverse-phase column (Luna C 8, Phenomenex, Torrance, CA, 150 × 4.6 mm, 3 μm particle size). The mobile phase was composed of A (0.05% formic acid in water) and B (acetonitrile) and ran from 5% B for 10 min to 100% B for 5 min or alternatively from 5 to 20% B for 10 min and then to 100% B for 5 min, at a flow rate of 1 mL/min. The eluate was monitored at 284 nm. The injection volume was 10 μL. Calibration straight lines were recorded in the concentration range of 4−100 μM for every 3(2*H*)-furanone ($R^2 > 0.9964$) and used for quantification (HDMF, $y = 1362x$, LOD = 0.02 ng/μL, LOQ = 0.10 ng/μL; DMMF, $y = 2127x$, LOD = 0.02 ng/μL, LOQ = 0.11 ng/μL; HDMF-glucoside, $y = 3695x$, LOD = 0.04 ng/μL, LOQ = 0.23 ng/μL; HEMF, $y = 1765x$, LOD = 0.02 ng/μL, LOQ = 0.11 ng/μL; HMF, $y = 2437x$, LOD = 0.01 ng/μL, LOQ = 0.06 ng/μL). Compounds were identified by their characteristic UV spectra (maxima between 276 nm for HDMF-glucoside and 285 nm for HDMF) and their retention times.

LC−MS Analysis. A Bruker Daltonics esquire 3000^{plus} ion trap mass spectrometer (Bruker Daltonics, Bremen, Germany) connected with an Agilent 1100 LC system (Agilent Technologies, Waldbronn, Germany) equipped with a quaternary pump and a variable wavelength detector was used. Components were separated with a Phenomenex (Aschaffenburg, Germany) Luna C-18 column (150 mm long × 2.0 mm inner diameter, particle size of 5 μm), which was held at 25 °C. Samples were analyzed using a linear gradient from 100% A (0.1% formic acid in water) to 20% B (acetonitrile) for 10 min and then to 100% B for 10 min, with a flow rate of 0.2 mL/min. Alternatively, a linear gradient from 5% B for 10 min and then to 100% B for 5 min was used. The detection wavelength was 285 nm. The electrospray ionization voltage of the capillary was set to −4000 V, and the end plate was set to −500 V. Nitrogen was used as a dry gas at a temperature of 330 °C and a flow rate of 9 L/min. The full-scan mass spectra were measured in a scan range from m/z 50 to 800 with a scan resolution of m/z 13 000 s^{-1} until the ICC target reached 20 000 or 200 ms, whatever was achieved first. Tandem mass spectrometry was carried out using helium as a collision gas (3.56×10^{-6} mbar), with the collision voltage set at 1 V. Spectra were acquired in the positive and negative ionization modes. Data analysis was performed using the Data Analysis 3.1 software (Bruker Daltonics, Bremen, Germany). The mass spectra of the furanones showed the expected pseudo-molecular $[M + H]^+$ and $[M + Na]^+$ ions (see Figure S1 in the Supporting Information).

Data Analysis. Reported values represent means ± standard deviation (SD) ($n = 6$).

RESULTS

Time Course of Transepithelial Transport. The basolateral uptake of apically applied solutions of HDMF, DMMF, HDMF-glucoside, HEMF, and HMF by Caco-2 cells was quantified over 4 h (**Figure 2**). The highest relative absorption was determined for the methyl ether DMMF, which reached 35% of the applied amount after 4 h and was, thus, twice as high as the relative absorption of HDMF. The absorption rates of HEMF and HMF corresponded to that of HDMF, while HDMF-glucoside was barely resorbed. Within the experimental period of 4 h, the uptake rates remained almost constant for the individual compounds. HDMF (68%), HEMF (65%), and HMF (78%) showed the lowest recovery values (total of apical and basolateral levels), whereas HDMF-glucoside (86%) and DMMF (101%) were almost completely recovered. LC analysis of the HDMF-, HEMF-, and HMF-containing solutions demonstrated the formation of additional compounds probably because of the instability of these 3(2*H*)-furanones (see Figure S2 in the Supporting Information). In a second series of experiments, two different levels of HDMF, DMMF, and HDMF-glucoside were apically applied to Caco-2 monolayers and the concentrations determined in the basolateral solutions after defined periods (**Figure 2c**). Over a time period of 24 h, the basolateral uptake of HDMF and DMMF showed a sigmoid curve for both levels. The transported rate decreased with an increasing incubation period. DMMF showed the highest resorption rate, and HDMF-glucoside was almost not absorbed. Except for HDMF, the uptake rates for the two

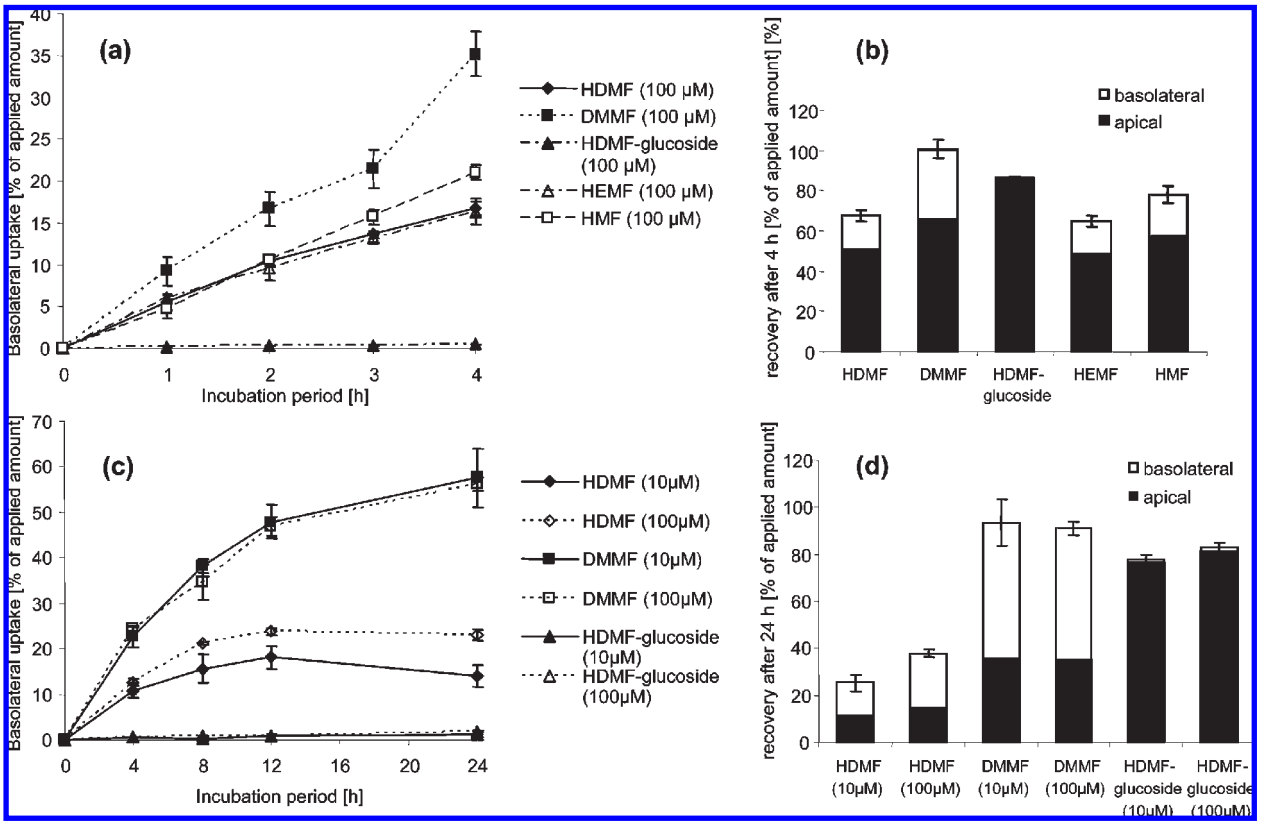

Figure 2. (a) Basolateral uptake of 100 μM solutions of HDMF, DMMF, HDMF-glucoside, HEMF, and HMF by Caco-2 cells over 4 h and (c) basolateral uptake of two different levels (10 and 100 μM) of HDMF, DMMF, and HDMF-glucoside over 24 h. Cells were incubated for 4 and 24 h with HDMF, DMMF, HDMF-glucoside, HEMF, and HMF. Samples taken from the basolateral side of the monolayers were analyzed by HPLC−DAD. Recovery of (b) HDMF, DMMF, HDMF-glucoside, HEMF, and HMF after 4 h and (d) HDMF, DMMF, and HDMF-glucoside after 24 h. After 4 and 24 h of incubation, samples were taken from the apical and basolateral sides of the monolayers and analyzed by HPLC−DAD.

concentrations used did not differ significantly. After the treatment of the cells for 24 h, the recovery values for HDMF further decreased to 26 and 38% for the 10 and 100 μM concentrations, respectively. DMMF (93 and 91%) and HDMF-glucoside (78 and 83%) are more stable and were almost completely retrieved (**Figure 2d**).

Concentration Dependency of 3(2*H*)-Furanone Transport. To test whether the transport of 3(2*H*)-furanones can be saturated by high levels, Caco-2 cells were apically incubated with 100 and 500 μM solutions of HDMF, DMMF, and HDMF-glucoside for 4 h. As a result, saturation of the transport was not observed (**Figure 3a**), although the relative transport of DMMF decreased when the 100 μM solution was replaced by the 500 μM concentration.

Reverse Transport. The 3(2*H*)-furanones were applied to the basolateral and apical sides of Caco-2 monolayers to test the option of a bidirectional transport. The transport of HDMF, DMMF, and HDMF-glucoside proceeded in the apical−basolateral and basolateral−apical directions because similar curves were obtained when the levels of the furanones in the basolateral and apical solutions were determined (**Figure 3b**). HDMF and HDMF-glucoside were transported in each direction with the same efficiency. After 4 and 8 h of treatment, Caco-2 cells showed the same uptake rates for DMMF in both directions. Longer treatment times of up to 24 h resulted in a decrease of the methyl ether transport from the basolateral to apical side in comparison to the reverse direction. Thus, the apical−basolateral transport of DMMF is more efficient than the return transport for treatment times longer than 8 h.

Uptake by Osmotic Gradient. The effect of apical hyperosmolarity was investigated to differentiate between trans- and paracellular transport by the Caco-2 monolayers. Mannitol was added to buffers containing the furanones, and uptake of the compounds by the cells was compared to the values obtained in control experiments without mannitol (**Figure 3c**). A slight reduction of the HDMF and DMMF transport was observed when the osmotic gradient was applied. However, HDMF-glucoside was better absorbed in the presence of mannitol. Prior to the treatment with HDMF and mannitol, Caco-2 cells neither differed in the morphological appearance nor in the TEER value. Also, after the incubation with HDMF, no difference was observed. The addition of mannitol changed the appearance of the cell layers significantly. The net structure of the monolayer was disrupted, and it appeared that some cells separated from the united cell structure. The TEER values determined after the experiment with mannitol were very low (346 Ω cm^2) compared to values obtained in the control study (452 Ω cm^2), although higher values were expected because of the hyperosmolarity.

Hydrolysis of HDMF-glucoside. Detailed analyses of the LC runs revealed the formation of small amounts of HDMF from HDMF-glucoside in apical samples. Identity of the liberated furanone was confirmed by DAD and electrospray ionization (ESI)−MS/MS analysis. Corresponding blanks and controls were used to ensure an enzymatic rather than chemical hydrolysis. Recovery of HDMF-glucoside reached almost 100% after 12 and 24 h when the hydrolysis of the glucoside was taken into account (**Figure 4a**). After 24 h, free HDMF amounted to about 9% of the initial molar HDMF-glucoside level. HDMF was also detected in the basolateral buffer. After 24 h, twice the amount of HDMF was taken up in comparison to the glucoside. To localize the site of the hydrolysis, HDMF-glucoside was added to the apical or basolateral side of Caco-2 cells or incubated for

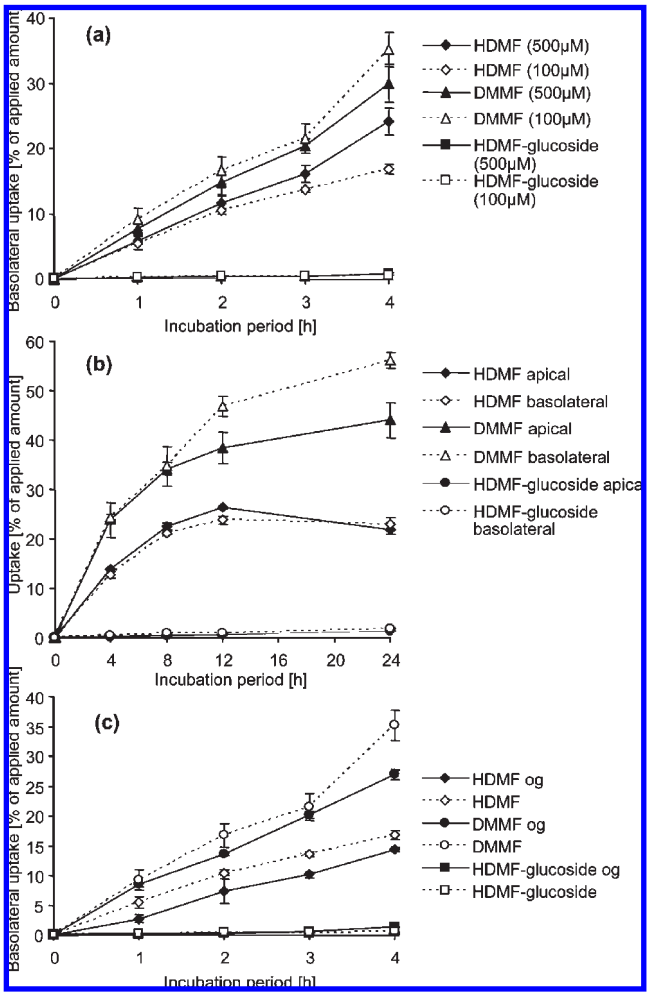

Figure 3. Uptake of HDMF, DMMF, and HDMF-glucoside by Caco-2 cells. (a) Basolateral uptake of 100 and 500 μM solutions. Cells were incubated with 100 and 500 μM solutions of the 3(2*H*)-furanones for 4 h. Samples were taken from the basolateral side. (b) Basolateral and apical transport within 24 h. Caco-2 monolayers were incubated with 100 μM of the 3(2*H*)-furanones from the basolateral (return transport) and apical sides. Samples were taken from the reverse side. (c) Basolateral uptake with and without osmotic gradient (og). Cells were incubated at the apical side with 100 μM solutions of the 3(2*H*)-furanones in buffer and buffer containing 100 mM mannitol (og). Compounds were quantified by HPLC−DAD.

4 h in pure buffer and buffer solutions that had been collected after 4 and 24 h from the apical and basolateral sides of the monolayers (**Figure 4b**). Hydrolysis of HDMF-glucoside was only observed in apical cell buffers. The level of liberated HDMF was significantly higher in the presence of cells, and the 24 h buffer exhibited a higher hydrolytic activity than the 4 h buffer.

DISCUSSION

In a previous human intervention trial, we demonstrated the high excretion rate of HDMF and identified HDMF-glucuronide as a major metabolite in urine (*19*). In this study, we investigated the uptake route and rates of the 3(2*H*)-furanones.

Uptake of 3(2*H*)-Furanones. DMMF showed the highest uptake rate in all experiments, while HDMF-glucoside had the lowest bioavailability. Free HDMF was about 90% more available than the glucoside. Similar results were obtained when the uptake rates of the flavonoids genistein and apigenin were compared to those of the corresponding glucosides (*23*). However, the absorption rates for HDMF were much lower

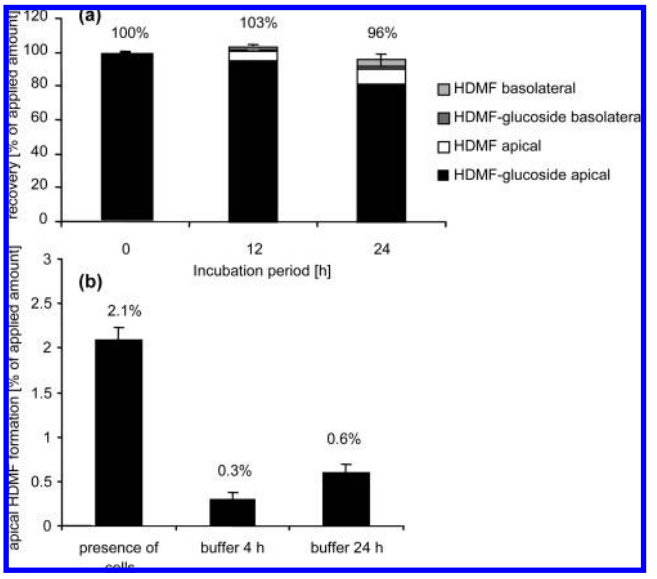

Figure 4. (a) Recovery of HDMF-glucoside after 12 and 24 h. Caco-2 cells were incubated with 100 μM HDMF-glucoside for 24 h. Samples were taken after 12 and 24 h from the apical and basolateral sides. (b) Apical HDMF release from HDMF-glucoside after 4 h. HDMF formation was quantified in apically applied buffer containing HDMF-glucoside (presence of cells) and buffer solutions that have been incubated with Caco-2 monolayers for 4 and 24 h and were then removed from the cells and supplemented with HDMF-glucoside.

than anticipated from the human intervention trial. With excretion rates of 60−90% of the orally applied amount as determined in the human study, comparable levels can be hypothesized to penetrate the small intestine. However, only about 17% of HDMF was taken up by the Caco-2 cell model after 4 h of incubation, which is a realistic absorption period. This value is by a factor of 5 lower than the rates determined in the human study. In contrast to DMMF, which was almost completely recovered from the buffer solutions, only about 30% of the initial HDMF concentration was recovered after 24 h of incubation. HDMF is prone to oxidation and heat (*24*, *25*). It is assumed that HDMF is either degraded at the brush border membrane enzymatically or chemically catalyzed in the cell buffer, which would explain the additional signals in the LC runs after 24 h of incubation (see Figure S2 in the Supporting Information). HEMF is similarly unstable, as demonstrated by the formation of new LC signals, and it shows comparable values for absorption and recovery (see Figure S2 in the Supporting Information). HMF was more stable, but highest recovery rates were obtained for DMMF and HDMF-glucoside, of which the hydroxyl group of HDMF is either methylated or glucosylated, respectively. Absorption in Caco-2 cells can be neglected because the HDMF and HEMF derivatives can explain parts of the missing amounts. Also, DMMF was completely recovered.

Paracellular Diffusion. Because the transport of 3(2*H*)-furanones could not be saturated by high levels of the substances and bidirectional transport was observed, a directed active transport is unlikely. It follows that the driving force of the diffusion is the concentration gradient between the apical and basolateral sides of the monolayer. The gradient and passive diffusion rate decrease with increasing incubation periods, as demonstrated by the sigmoid uptake curve. The 3(2*H*)-furanones are highly polar molecules that cannot transcellularly pass the phospholipid bilayer but are small enough to penetrate the hydrophilic pores of the tight junctions (*26*). HDMF-glucoside

is significantly larger than the free furanones, which would explain the low absorption via paracelluar diffusion. Although the transport of HDMF and DMMF was inhibited by the application of apical hyperosmolarity, which is in accordance with the assumption of paracellular diffusion, the effect was lower than anticipated. Microscopic analysis after the experiments of the monolayer showed that some of the cell−cell junctions were disrupted, which accounts for the unexpected reduction of the TEER value. The enhanced transport of HDMF-glucoside also confirmed the increased paracellular permeability in the presence of 100 mM mannitol. Finally, because Caco-2 cells form less permeable tight junctions than small-intestine epithelial cells *in vivo*, it is conceivable that the absorption rate of furanones in Caco-2 cell layers is significantly lower compared to that indicated by the results from human intervention trials (*19*, *27*). This hypothesis is in accordance with results reported for other paracellularly transported molecules, such as metformin and atenolol, for which the absorption rate in a human study was 50% higher than that in cultured Caco-2 cells (*28*).

Hydrolysis of HDMF-glucoside. Our experiments confirm the hydrolytic degradation of HDMF-glucoside prior to absorption. The respective enzymes are probably located in the brush border membrane because the highest hydrolysis rates were observed in the presence of Caco-2 cells. It has already been shown that the membrane-bound lactase, which is expressed in Caco-2 cells, catalyzes also the hydrolysis of β-glucosides (*22*). Hydrolysis in the cell buffers is likely performed by lactase released from enterocytes. However, enzymatic hydrolysis liberated only 2% of the applied amount of the glucoside as HDMF. This result is in contrast to the values obtained in a human study, where 60−90% of the orally applied levels of HDMF, DMMF, and HDMF-glucoside were excreted as glucuronide and sulfate (*19*). Similarly, Caco-2 cells showed lower hydrolysis rates for flavonoid glucosides in comparison to a perfused rat intestinal model (*23*, *27*). Therefore, it seems likely that lactase is not highly expressed in Caco-2 cells. Because hydrolysis of β-glucosides in the upper gastrointestinal tract can be ignored, it is conceivable that the bacterial gut flora releases most of the aglycon from its glycoside, as already shown for naringenin-7-rhamnoglucoside in mice (*29*).

Intestinal Metabolism. HDMF-glucuronide and -sulfate were not detected in the samples, although enterocyctes express phase I and II enzymes. This observation, however, confirms the paracellular diffusion of the 3(2*H*)-furanones, which are therefore not available as substrates for intracellular glucuronosyl and sulfate transferases. The high levels of HDMF-glucuronide observed in urine of healthy volunteers probably originated in the liver, where phase I and II enzymes are highly expressed (*19*).

The Caco-2 cell model is one of the best characterized transport models, although it shows some weaknesses, such as low paracellular diffusion rates because of less permeable tight junctions and low expression rates for lactase (*27*). Thus, uptake and hydrolysis of food ingredients are much higher *in vivo* than determined in the Caco-2 system. The chemical degradation of HDMF during the 24 h incubation period is irrelevant for the *in vivo* situation, where mean absorption periods of 4−6 h are assumed. Finally, the complexity of the food matrix cannot be studied in cultured cells because specific molecules, such as capsianosides in pepper, can weaken the tight junction and increase the paracellular permeability (*30*, *31*). In conclusion, 3(2*H*)-furanones are transported through the epithelial cell layer by passive diffusion, whereby HDMF-glucoside passes through Caco-2 monolayers much less efficiently than HDMF, HEMF, HMF, and DMMF. It is likely that hydrolysis of the glucoside to its aglycone by enterobacteria is required for effective absorption in the intestinal tract.

ACKNOWLEDGMENT

The authors thank Roland Rabeler, Michaela Thalhammer, and Hans-Ullrich Hoppe for providing the Caco-2 cells and the equipment for the cell-culture experiments.

Supporting Information Available: MS/MS analysis of HDMF-glucoside (Figure S1) and HPLC−DAD analysis of the apical HEMF sample after 4 h and the apical HDMF sample after 24 h (Figure S2). This material is available free of charge via the Internet at http://pubs.acs.org.

LITERATURE CITED

(1) Slaughter, J. C. The naturally occurring furanones: Formation and function from pheromone to food. *Biol. Rev*. **1999**, *74*, 259–276.
(2) Raab, T.; López-Ráez, J. A.; Klein, D.; Caballero, J. L.; Moyano, E.; Schwab, W.; Muñoz-Blanco, J. *FaQR*, required for the biosynthesis of the strawberry flavor compound 4-hydroxy-2,5-dimethyl-3(2*H*)-furanone, encodes an enone oxidoreductase. *Plant Cell* **2006**, *18*, 1023–1037.
(3) Hayashida, Y.; Nishimura, K.; Slaughter, J. C. The importance of the furanones HDMF and HEMF in the flavour profile of Japanese barley miso and their production during fermentation. *J. Sci. Food Agric*. **1998**, *78*, 88–94.
(4) Newman, L. M.; Garcia, H.; Hudlicky, T.; Selifonov, S. A. Directed evolution of the dioxygenase complex for the synthesis of furanone flavour compounds. *Tetrahedron* **2004**, *60*, 729–734.
(5) Schwab, W.; Davidovich-Rikanati, R.; Lewinsohn, E. Biosynthesis of plant-derived flavor compounds. *Plant J*. **2008**, *54*, 712–732.
(6) Hiramoto, K.; Aso-o, R.; Ni-iyama, H.; Hikage, S.; Kato, T.; Kikugawa, K. DNA strand break by 2,5-dimethyl-4-hydroxy-3(2*H*)-furanone, a fragrant compound in various foodstuffs. *Mutat. Res*. **1996**, *359*, 17–24.
(7) Hiramoto, K.; Sekiguchi, K.; Ayuha, K.; Aso-o, R.; Moriya, N.; Kato, T.; Kikugawa, K. DNA breaking activity and mutagenicity of soy sauce: Characterization of the active components and identification of 4-hydroxy-5-methyl-3(2*H*)-furanone. *Mutat. Res*. **1996**, *359*, 119–132.
(8) Yasumoto, E.; Nakano, K.; Nakayachi, T.; Morshed, S. R.; Hashimoto, K.; Kikuchi, H.; Kawase, M.; Sakagami, H. Cytotoxic activity of deferiprone, maltol and related hydroxyketones against human tumor cell lines. *Anticancer Res*. **2004**, *24*, 755–762.
(9) Li, X.; Hiromoto, K.; Yoshida, M.; Kato, T.; Kikugawa, K. Identification of 2,5-dimethyl-4-hydroxy-3(2*H*)-furanone (DMHF) and 4-hydroxy-2(or 5)-ethyl-5(or 2)-methyl-3(2*H*)-furanone (HEMF) with DNA breaking activity in soy sauce. *Food Chem. Toxicol*. **1998**, *36*, 305–314.
(10) Yamashita, N.; Murata, M.; Inoue, S.; Hiraku, Y.; Yoshinaga, T.; Kawanishi, S. Superoxide formation and DNA damage induced by a fragrant furanone in the presence of copper(II). *Mutat. Res*. **1998**, *397*, 191–201.
(11) Murakami, K.; Haneda, M.; Makino, T.; Yoshino, M. Prooxidant action of furanone compounds: Implication of reactive oxygen species in the metal-dependent strand breaks and the formation of 8-hydroxy-2′-deoxyguanosine in DNA. *Food Chem. Toxicol*. **2007**, *45*, 1258–1262.
(12) Nagahara, A.; Benjamin, H.; Storkson, J.; Krewson, J.; Sheng, K.; Liu, W.; Pariza, M. W. Inhibition of benzo[α]pyrene-induced mouse forestomach neoplasis by a principal flavor component of Japanese-style fermented soy sauce. *Cancer Res*. **1992**, *52*, 1754–1756.
(13) Kataoka, S.; Liu, W.; Albright, K.; Storkson, J.; Pariza, M. Inhibition of benzo[*a*]pyrene-induced mouse forestomach neoplasia and reduction of H_2O_2 concentration in human polymorphonuclear leucocytes by flavour components of Japanese-style fermented soy sauce. *Food Chem. Toxicol*. **1997**, *35*, 449–457.

(14) Sasaki, T.; Yamakoshi, J.; Saito, M.; Kasai, K.; Matsudo, T.; Koga, T.; Mori, K. Antioxidative activities of 4-hydroxy-3(2*H*)-furanones and their anti-cataract effect on spontaneous cataract rat (ICR/f). *Biosci., Biotechnol., Biochem*. **1998**, *62*, 1865–1869.

(15) Koga, T.; Moro, K.; Matsudo, T. Antioxidative behaviours of 4-hydroxy-2,5-dimethyl-3(2*H*)-furanone and 4-hydroxy-2(or 5)-ethyl-5(or 2)-methyl-3(2*H*)-furanone against lipid peroxidation *J. Agric. Food Chem*. **1998**, *46*, 946–951.

(16) Sang, S. W.; Jung, H. J.; Lee, I. S.; Kim, H. S.; Lee, D. G. Antimicrobial effect of furaneol against human pathogenic bacteria and fungi. *J. Microbiol. Biotechnol*. **2006**, *16*, 349–354.

(17) Kikugawa, K.; Hiramoto, K.; Matsumoto, H.; Kato, T. Fragrant 4-hydroxy-3(2*H*)-furanones swiftly scavenge nitrous acid causing concomitant formation of the components with relatively weak mutagenicity. *J. Health Sci*. **2000**, *46*, 35–41.

(18) Li, S.; Li, K.; Zh, X. The absorption, distribution, and excretion of 4-hydroxy-2,5-dimethyl-3(2*H*)-furanone in rats. *Zhonghua Laodong Weisheng Zhiyebing Zazhi* **1990**, *8*, 172–173.

(19) Roscher, R.; Koch, H.; Herderich, M.; Schreier, P.; Schwab, W. Identification of 2,5-dimethyl-4-hydroxy-3(2*H*)-furanone-β-D-glucuronide as the major metabolite of a strawberry flavour constituent in humans. *Food Chem. Toxicol*. **1997**, *35*, 777–782.

(20) Mayerl, F.; Naf, R.; Thomas, A. F. 2,5-Dimethyl-4-hydroxy-3(2*H*)-furanone glucosides: Isolation from strawberries and synthesis. *Phytochemistry* **1989**, *28*, 631–633.

(21) Hidalgo, I. J.; Raub, T. J.; Borchardt, R. T. Characterization of the human colon carcinoma cell line (Caco-2) as a model system for intestinal epithelial permeability. *Gastroenterology* **1989**, *96*, 736–749.

(22) Quaroni, A.; Hochman, J. Development of intestinal cell culture models for drug transport and metabolism studies. *Adv. Drug Delivery Rev*. **1996**, *22*, 3–52.

(23) Liu, Y.; Hu, M. Absorption and metabolism of flavanoids in the Caco-2 cell culture model and a perfused rat intestinal model. *Drug Metab. Dispos*. **2001**, *30*, 370–377.

(24) Rowe, D. Fun with furans. In *Perspectives in Flavor and Fragrance Research*; Kraft, P., Swift, K. A. D., Eds.; Wiley-VCH: Weinheim, Germany, 2005; pp 207−214.

(25) Roscher, R.; Schwab, W.; Schreier, P. Stability of naturally occurring 2,5-dimethyl-4-hydroxy-3[2*H*]-furanone derivatives. *Eur. Food Res. Technol*. **1997**, *204*, 438–441.

(26) Knipp, G. T.; Ho, N. F. H.; Barsuhn, C. L.; Borchardt, R. T. Paracellular diffusion in Caco-2 cell monolayers: Effect of perturbation on the transport of hydrophilic compounds that vary in charge and size. *J. Pharm. Sci*. **2000**, *86*, 1105–1110.

(27) Ingels, F. M.; Augustijns, P. F. Biological, pharmaceutical, and analytical considerations with respect to the transport media used in the absorption of screening system, Caco-2. *J. Pharm. Sci*. **2003**, *92*, 1545–1558.

(28) Balimane, P. V.; Chong, S. Cell culture-based models for intestinal permeability: A critique. *Drug Discovery Today* **2005**, *10*, 335–343.

(29) Felgines, C.; Texier, O.; Morand, C.; Manach, C.; Scalbert, A.; Regerat, F.; Remesy, C. Bioavailability of the flavanone naringenin and its glycosids in rats. *Am. J. Physiol.: Gastrointest. Liver Physiol*. **2000**, *279*, G1148–G1154.

(30) Shimizu, M. Modulation of intestinal functions by food substances. *Nahrung* **1999**, *43*, 154–158.

(31) Konishi, Y. Modulations of food-derived substances on intestinal permeability in Caco-2 cell monolayers. *Biosci,. Biotechnol., Biochem*. **2003**, *67*, 2297–2299.

Received for Review January 16, 2009. Revised manuscript received March 12, 2009. Accepted March 17, 2009. Degussa AG is acknowledged for financial support.